

Cluster-glass phase in pyrochlore XY antiferromagnets with quenched disorder

Eric C. Andrade,¹ José A. Hoyos,¹ Stephan Rachel,^{2,3} and Matthias Vojta²

¹*Instituto de Física de São Carlos, Universidade de São Paulo, C.P. 369, São Carlos, SP, 13560-970, Brazil*

²*Institut für Theoretische Physik, Technische Universität Dresden, 01062 Dresden, Germany*

³*School of Physics, University of Melbourne, Parkville, VIC 3010, Australia*

(Dated: April 6, 2024)

We study the impact of quenched disorder (random exchange couplings or site dilution) on easy-plane pyrochlore antiferromagnets. In the clean system, order-by-disorder selects a magnetically ordered state from a classically degenerate manifold. In the presence of randomness, however, different orders can be chosen locally depending on details of the disorder configuration. Using a combination of analytical considerations and classical Monte-Carlo simulations, we argue that any long-range-ordered magnetic state is destroyed beyond a critical level of randomness where the system breaks into magnetic domains due to random exchange anisotropies, becoming, therefore, a glass of spin clusters, in accordance with the available experimental data. These random anisotropies originate from off-diagonal exchange couplings in the microscopic Hamiltonian, establishing their relevance to other magnets with strong spin-orbit coupling.

Rare-earth pyrochlores form one of the most interesting families of frustrated magnets. A lattice of corner-sharing tetrahedra combined with a multiplicity of crystal-field effects for rare-earth ions [1] gives rise to a plethora of novel states [2]. Among them are disordered spin ices [3–6] and quantum spin liquids [7–9], found in materials with magnetic easy-axis anisotropy. In contrast, compounds exhibiting an easy-plane (or XY) anisotropy tend to order antiferromagnetically [10–16]. A number of them realize an “order-by-disorder” mechanism where a long-range-ordered state is selected, via either thermal or quantum fluctuations, from a classically degenerate manifold resulting from strong frustration [12, 17–19]. In the parameter regime relevant to the paradigmatic example $\text{Er}_2\text{Ti}_2\text{O}_7$, both classical and quantum fluctuations select the noncoplanar state dubbed ψ_2 from a one-parameter manifold, in a remarkable agreement with experiments [11, 12].

Quenched disorder provides a different route for lifting the classical degeneracy by locally relieving the frustration [20]. Previous theoretical studies showed that both bond randomness and site dilution tend to stabilize, for small disorder, the coplanar state dubbed ψ_3 [21, 22]. This insight motivated a series of experiments in inhomogeneous XY pyrochlore magnets. In $\text{Er}_{2-x}\text{Y}_x\text{Ti}_2\text{O}_7$ [23] magnetic Er^{3+} is substituted by nonmagnetic Y^{3+} , corresponding to site dilution. For $\text{NaCaCo}_2\text{F}_7$ [24, 25] and $\text{NaSrCo}_2\text{F}_7$ [26] quenched disorder arises from site mixing on the pyrochlore A sites (Na/Ca and Na/Sr, respectively), with the leading effect on magnetism being bond randomness. However, all experiments find either the ψ_2 state, for small disorder, or short-range magnetic correlations below a freezing temperature T_f at stronger disorder, suggesting a spin-glass state.

In this Letter, we solve this puzzle. We develop a more general theory, valid in the experimentally relevant regime, showing that disorder-induced random anisotropies destabilize magnetic long-range order (LRO)

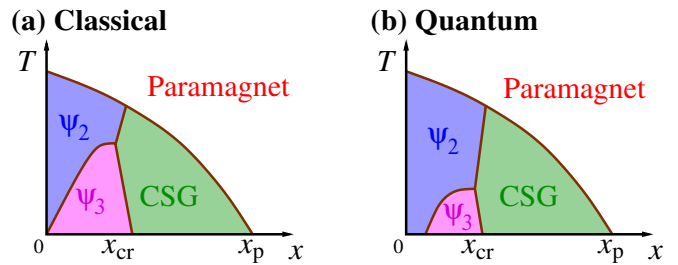


Figure 1. (Color online) Schematic phase diagram for the easy-plane pyrochlore antiferromagnet (1) as function of temperature T and site dilution x , for parameters with $0 < J_{\pm\pm}/J_{\pm} \leq 2$ where order-by-disorder selects the ψ_2 state in the clean limit, $x=0$. Quenched disorder tends to select the ψ_3 state at low T , but both $\psi_{2,3}$ are destroyed beyond a critical level of disorder x_{cr} where randomness breaks the system into magnetic domains resulting in a cluster spin glass (CSG) phase which survives up to the percolation threshold x_p . (a) Without quantum fluctuations, i.e., in the classical limit. (b) With quantum fluctuations. Here ψ_3 may disappear completely, for details see text.

of easy-plane pyrochlores. We derive a semi-quantitative stability criterion which indicates that LRO is destroyed beyond a critical level of quenched disorder. Using extensive Monte-Carlo (MC) simulations for the relevant classical model, we verify the tendency towards ψ_3 order in the weakly diluted regime [21, 22], and provide compelling evidence that the low- T state at stronger disorder is a cluster spin-glass (CSG) phase where the system breaks into domains (spins clusters) exhibiting a variety of *local* ordering patterns besides the ψ_2 and ψ_3 ones. For the quantum case, we argue that the tendency towards ψ_3 order is diminished, such that a significant portion of the phase diagram is dominated by the CSG phase, Fig. 1, in agreement with available experiments.

Model.— The low-temperature properties of many rare-earth insulating pyrochlore oxides are well described by an effective spin-1/2 model with anisotropic exchange

interactions due to the combination of spin-orbit and crystalline electric-field effects [1]. In $\text{Er}_2\text{Ti}_2\text{O}_7$, for instance, the spins have a dominant planar nature, and the associated nearest-neighbor anisotropic XY model [8, 11, 12, 27, 28] can be written as

$$\mathcal{H} = - \sum_{\langle jk \rangle} \left[J_{jk}^{xx} S_j^x S_k^x + J_{jk}^{yy} S_j^y S_k^y + J_{jk}^{xy} (S_j^x S_k^y + S_j^y S_k^x) \right]. \quad (1)$$

Here, the sum runs over pairs of nearest-neighbor (NN) sites on a cubic pyrochlore lattice, the couplings are

$$J_{jk}^{xx(yy)} = 2(J_{jk}^{\pm} \mp J_{jk}^{\pm\pm} \cos\theta_{jk}), \quad J_{jk}^{xy} = 2J_{jk}^{\pm\pm} \sin\theta_{jk}, \quad (2)$$

and the spin components $S^{x,y}$ are written in the local coordinate reference frames (one for each of the four sublattices) which are confined to planes perpendicular to the local $\langle 111 \rangle$ axes. J^{\pm} and $J^{\pm\pm}$ are the symmetry-allowed NN exchange couplings [8, 12, 29]. We adopt the choice of the local frames as in Refs. 21 and 25, with the corresponding angular phases (inside a tetrahedron of sites labeled from 0 to 3) $\theta_{01} = \theta_{23} = 0$, $\theta_{02} = \theta_{13} = 2\pi/3$, and $\theta_{03} = \theta_{12} = -2\pi/3$.

In the clean limit, and for $-2 < \alpha \equiv J^{\pm\pm}/J^{\pm} < 2$, the mean-field ground states of (1) are given by spins collectively pointing along any direction in the XY plane, exhibiting a continuous $U(1)$ degeneracy with energy $E_0/J^{\pm} = -6NS^2$. The order-by-disorder mechanism selects a finite set of six states out of the degenerate manifold: for $0 < \alpha < 2$ ($-2 < \alpha < 0$) the ψ_2 (ψ_3) state is selected which corresponds to spins pointing along one of the $\cos(\frac{\pi}{3}n)\hat{x} + \sin(\frac{\pi}{3}n)\hat{y}$ ($\cos(\frac{\pi}{3}n + \frac{\pi}{6})\hat{x} + \sin(\frac{\pi}{3}n + \frac{\pi}{6})\hat{y}$) directions, with $n = 0, \dots, 5$, in the local reference frame [11, 12].

For definiteness, we introduce quenched disorder via

$$J_{jk}^{\pm} = J^{\pm} (1 + \epsilon_{jk}), \quad J_{jk}^{\pm\pm} = J^{\pm\pm} (1 + \epsilon_{jk}), \quad (3)$$

where ϵ_{jk} are random variables. Bond disorder corresponds to ϵ_{jk} drawn independently from some distribution, while site dilution yields $\epsilon_{jk} = -1$ if either site j or site k hosts a vacancy and $\epsilon_{jk} = 0$ otherwise. Site dilution is parameterized by the concentration x of non-magnetic impurities; for bond randomness see [30].

Destruction of order by random-fields effects.— We adopt a transparent argument by Aharony, originally constructed to show the instability of an ordered magnetic state against weak random anisotropy [31].

We assume LRO which is uniform in the local frames of the Hamiltonian (1), with $|\alpha| < 2$, such that $\langle \mathbf{S} \rangle = \langle S^x \rangle \hat{x} + \langle S^y \rangle \hat{y} = m \hat{n}_{\parallel}$ where $\langle \dots \rangle$ denotes the thermal average. The corresponding local exchange field is $\mathbf{h}_j = \sum_{k=1}^z (J_{jk}^{xx} \langle S^x \rangle + J_{jk}^{xy} \langle S^y \rangle) \hat{x} + (J_{jk}^{yy} \langle S^y \rangle + J_{jk}^{yx} \langle S^x \rangle) \hat{y}$, with the sum running over all the $z = 6$ NN sites. In the presence of random off-diagonal disorder the local exchange field $\mathbf{h}_j = h_j^{\parallel} \hat{n}_{\parallel} + h_j^{\perp} \hat{n}_{\perp}$ is not parallel to the mean magnetization. If we assume, for instance, $\langle S^x \rangle = \frac{1}{2}$

(and $\langle S^y \rangle = 0$) the local transverse component stems from the coupling J_{jk}^{xy} in (1), and is simply given by $h_j^{\perp}/J^{\pm\pm} = \sum_{k=1}^6 \epsilon_{jk} \sin\theta_{jk}$, see also Eqs. (2) and (3).

The random transverse field h_j^{\perp} [32] tips the local magnetization away from the mean direction \hat{n}_{\parallel} . The resulting transverse magnetization can be estimated in linear response as $\langle S_j^{\perp} \rangle = \sum_k \chi_{jk}^{\perp} h_k^{\perp}$ where χ_{jk}^{\perp} is the transverse bulk susceptibility of the clean system. The disorder-averaged transverse magnetization, $\overline{\langle S_j^{\perp} \rangle}$, vanishes because h_j^{\perp} has zero mean. In contrast, the averaged magnetization correlation function is non-zero: $\overline{\langle S_i^{\perp} S_j^{\perp} \rangle} \propto (\delta h)^2 \int d^d q (\chi^{\perp}(\mathbf{q}))^2 e^{i\mathbf{q} \cdot \mathbf{r}_{ij}}$ where $(\delta h)^2 \equiv \overline{h_i^{\perp 2}} > 0$ [33] and $d = 3$ the number of space dimensions. Further, $\chi^{\perp}(\mathbf{q}) \sim 1/(\lambda + \kappa_{\mu} q_{\mu}^2)$ is the Fourier-transformed bulk susceptibility, with λ being an effective anisotropy energy, such that the gap $\Delta \propto \sqrt{\lambda}$, and κ_{μ} parameterizing the gradient expansion [12, 30].

Importantly, if the anisotropy energy λ were zero, we would have $\chi^{\perp}(\mathbf{q}) \propto q^{-2}$, such that the local transverse magnetization fluctuations diverge for $d \leq 4$: These fluctuations, arising from random off-diagonal exchange interactions and transmitted by long-wavelength modes, then destroy the assumed ordered state. This destruction of LRO can also be interpreted in terms of breaking the system into domains of linear size ℓ , following Imry and Ma [34]. Consider domains inside which the transverse exchange fields $\{h_j^{\perp}\}$ are atypically strong, such that the local order parameter will align with it, gaining an energy scaling as $\delta h \ell^{d/2}$ (as dictates the central limit theorem). In addition, there is a domain-wall energy cost. $\lambda \rightarrow 0$ implies an (accidental) continuous symmetry, hence the order parameter can be continuously distorted from the \hat{n}_{\parallel} to the \hat{n}_{\perp} direction (in a region of fractions of ℓ), yielding a domain wall energy which scales as $J^{\pm} \ell^{d-2}$. Thus, for $d < 4$ it is favorable to break the system into domains of linear size $\ell \gtrsim (J^{\pm}/\delta h)^{2/(4-d)}$.

If, instead, the anisotropy energy λ is finite, the divergence is cured. Then the transverse spin fluctuations $\overline{\langle S_i^{\perp 2} \rangle}$ remain small for small δh , i.e., the assumed LRO is stable against weak randomness. A stability criterion can be obtained by the condition $\overline{\langle S_i^{\perp 2} \rangle} \ll 1$. This yields

$$\delta h \ll \kappa^{d/4} \lambda^{1-d/4} \quad (4)$$

up to numerical prefactors [30] where $\kappa^2 = \sum_{\mu} \kappa_{\mu}^2/3$. The criterion (4) is consistent with the fact that small randomness destroys LRO in the limit $\lambda \rightarrow 0$ for $d < 4$, but not for $d > 4$. δh grows with increasing randomness, and hence we expect, for $\lambda > 0$ and $d = 3$, the destruction of LRO beyond a critical level of randomness. Below we show that the resulting phase is a CSG. Importantly, this argument is rather general, not restricted to the specific choice of Eq. (1), since it relies only on the existence of an off-diagonal exchange coupling [31].

Effective anisotropy and critical disorder.— Without

quenched disorder, the system selects the ψ_2 state (for $0 < \alpha < 2$), with the spin gap Δ generated by the order-by-disorder mechanism [11, 12, 35]. Hence, λ is generically finite, and the ψ_2 state is stable against weak randomness, i.e., small δh . Indeed, a perturbation generated by a single defect is expected to be screened in the presence of a gap, such that a small concentration of defects does not qualitatively change the bulk state [21, 22].

Importantly, in the classical limit the ψ_2 gap arises exclusively from thermal fluctuations, hence $\Delta \rightarrow 0$ as $T \rightarrow 0$. Quenched disorder tends to stabilize the ψ_3 state instead [21, 22], with the effective anisotropy energy λ scaling linearly with x [21]. Hence, the putative ψ_3 state has $\lambda \propto x$ as $T \rightarrow 0$. As we show in Ref. 30, the fluctuating transverse field follows $\delta h \propto \sqrt{x}$, such that the criterion (4) is parametrically fulfilled for small x , but can be expected to be violated at larger x . We conclude that, in the classical limit and at low T , the ψ_3 state is stable in a window $0 < x < x_{\text{cr}}$, but replaced by a CSG for $x > x_{\text{cr}}$. The quantum case is more involved and will be discussed later.

Classical phase diagram.— We are now in the position to discuss the classical phase diagram of the model (1). As originally explained in Refs. 21 and 22, the behavior at small x is governed by the competition between ψ_2 and ψ_3 LRO, favored by thermal fluctuations and weak disorder, respectively. This results in a phase boundary varying linearly with x . With increasing x , random-field effects grow, and LRO is eventually destroyed in favor of a CSG at all T . The low- T competition between ψ_3 and CSG is based on energetics, such that their phase boundary depends weakly on x at low T . Further, the effective anisotropy λ is particularly small near the ψ_2 - ψ_3 boundary, and this is where CSG will win first upon increasing x . Together, these considerations yield the qualitative phase diagram in Fig. 1(a), and they are well borne out by our quantitative numerical simulations, Fig. 2.

Classical MC simulations.— We turn to a detailed analysis of the state at large disorder. Previous theoretical investigations of related cases [36–38] suggest a glassy state: The system breaks into domains of size ℓ , exhibiting no long-range magnetism, and eventually freezes into a spin glass below a temperature T_f . This scenario is in accordance with available experimental results for the random XY pyrochlores [23–26], and we now provide numerical evidence for it in the classical limit [39].

We perform classical MC simulations of the model (1) in the presence of site dilution and bond randomness [30]. Interpreting the simulation results requires care due to the several length scales present in the problem. In the clean limit, besides the linear system size L , there is an emergent length $\Lambda(T)$ [40, 41] associated to a dangerously irrelevant \mathbb{Z}_6 anisotropy [13]. Therefore, the ground-state selection only takes place for $L \gg \Lambda$; to observe this numerically requires either low T or large L . With quenched disorder there is yet another length scale, the domain size

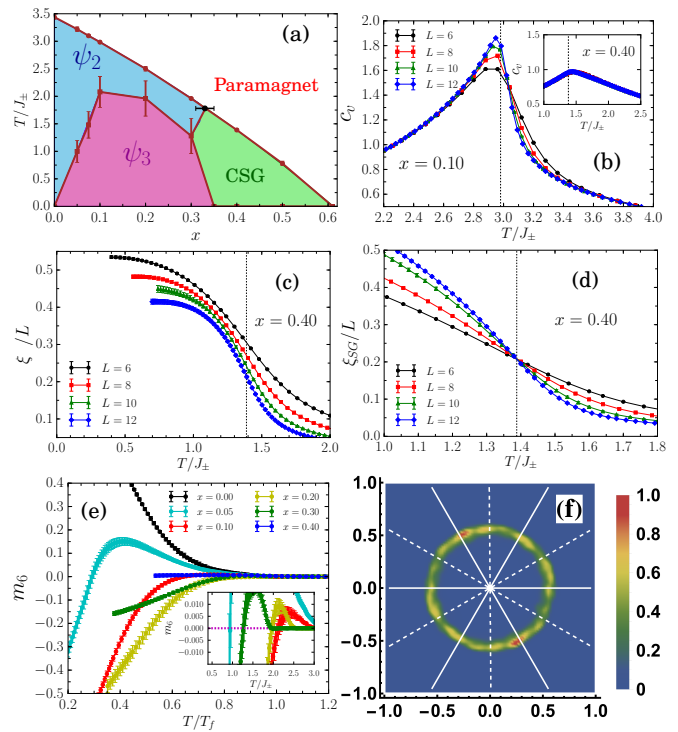


Figure 2. (Color online) Classical MC results for the Hamiltonian (1) for off-diagonal exchange ratio $\alpha = 1$. (a) Phase diagram as in Fig. 1. The freezing temperature T_f vanishes at the percolation threshold $x_p = 0.61$; the black dot marks the transition between ψ_2 and CSG, for details see text. (b) Specific heat $c_v(T)$ for $x = 0.1$ and $x = 0.4$ (inset). The vertical dashed line marks T_f . (c) Magnetic correlation length, plotted as $\xi^\perp(T)/L$, for $x = 0.4$ showing no crossing points. (d) Spin-glass correlation length, plotted as $\xi_{\text{SG}}(T)/L$, for $x = 0.4$ showing a crossing point at $T_f/J_\pm = 1.39(2)$. (e) Clock order parameter m_6 as a function of T/T_f for $L = 10$ and several values of x . Inset: zoom around the region where m_6 changes sign. (f) Sample-to-sample distribution $P(m_x, m_y)$ at $T = T_f/2$ for $x = 0.4$ and $L = 12$. The full (dashed) radial lines show the expected positions of the peaks associated to the $\psi_{2(3)}$ states.

ℓ , and we require $L \gg \ell$ to observe domain formation.

To monitor the order in the local XY planes we compute $m_{x(y)} = N^{-1} \sum_{j=1}^N S_j^{x(y)}$. The magnetic order parameter is $m = (m_x^2 + m_y^2)^{1/2}$, and we define an associated correlation length ξ^\perp . To discriminate between the states ψ_2 and ψ_3 we define a clock-like order parameter $m_6 = m \cos(6\varphi)$, where $\varphi = \tan^{-1}(m_y/m_x)$, with m_6 being positive (negative) for the $\psi_{2(3)}$ states. Moreover, we also keep track of the order-parameter distribution $P(m_x, m_y)$ [13, 40, 41], which is obtained considering statistics from different samples. In order to study spin-glass freezing we use the spin-glass (Edwards-Anderson) order parameter $q^{\alpha,\beta}(\mathbf{p}) = N^{-1} \sum_j S_j^{\alpha(1)} S_j^{\beta(2)} e^{i\mathbf{p}\cdot\mathbf{r}_j}$, where α and β are spin components, and (1) and (2) denote two identical copies of the system (“replicas”)

containing the same defect configuration. We define the spin-glass correlation length ξ_{SG} from this order parameter [42], and the freezing temperature T_f is obtained locating the crossing point of $\xi_{\text{SG}}(T)/L$ for different system sizes L . Note that the Edwards-Anderson parameter alone does not differentiate spin glass from LRO [30].

In the following we focus on the case of site dilution relevant, e.g., to the compound $\text{Er}_{2-x}\text{Y}_x\text{Ti}_2\text{O}_7$ [23]; bond randomness is discussed in Ref. 30. Sample results are presented in Fig. 2. We confirm the tendency towards ψ_3 order at low T and small x , see Figs. 2(b) and (e) for $x = 0.1$, in accordance with earlier simulations [21, 22]. We determine the transition from ψ_2 to ψ_3 as the point where the curve $m_6(T)$ changes sign for $L = 12$, see inset of Fig. 2(e). On general grounds, we expect this transition to be first order. However, we find no traces of it in the specific heat, as also reported in Refs. [21, 43], a fact which contributes to the error bars in Fig. 2(a). We leave a more detailed investigation of this point for future work.

For larger $x \gtrsim 0.3$ the behavior becomes more glassy: This is seen in the specific-heat curves, i.e., the maxima for all L become broad and size-independent, signaling the building up of short-range magnetic correlations above a freezing temperature T_f [44], Fig. 2(b). Moreover, the correlation-length data $\xi^\perp(T)/L$ do not display crossing points, Fig. 2(c), whereas $\xi_{\text{SG}}(T)/L$ show well-defined crossing points, Fig. 2(d). This signals glassy freezing in the *absence* of LRO. The freezing temperature $T_f(x)$ decreases with x , but remains finite up to the percolation threshold, $x_p = 0.61$, Fig. 2(a). The fate of the system is best judged by considering m_6 and the distribution $P(m_x, m_y)$, Figs. 2(e) and (f). m_6 is essentially zero for $x \gtrsim 0.4$, and $P(m_x, m_y)$ is peaked along a circle (instead of displaying sharp maxima), suggesting coexisting finite domains with distinct local spin orientations. We consider these MC data as clear evidence for the breaking of the system into domains with frozen spin configurations and no LRO, i.e., a CSG – this is the central result of this letter.

The transition from $\psi_{2,3}$ to the CSG can be determined from the absence both of crossing points in $\xi^\perp(T)/L$ and of a clear-cut temperature trend of m_6 . The resulting quantitative phase diagram is in Fig. 2(a), in remarkable agreement with the qualitative considerations which led to Fig. 1(a).

Quantum effects.— Turning to the quantum case, we note that the main effect of quantum fluctuations is to stabilize ψ_2 even at $T = 0$. This makes ψ_2 more competitive against ψ_3 and shifts the corresponding boundary to finite x [21]. As the competition between ψ_3 and CSG is expected to be weakly affected by quantum fluctuations, the extent of the ψ_3 phase consequently shrinks, Fig. 1(b). For strong quantum effects, $S = 1/2$, we may speculate that ψ_3 disappears completely from the phase diagram, yielding a direct transition from ψ_2 to CSG for

all temperatures below T_f , but this requires a more detailed and quantitative analysis of quantum effects which is beyond the scope of this paper.

Experiments.— We now confront our theory with experimental data. Assuming that $m = \langle S^x \rangle = \frac{1}{2}$ and $\langle S^y \rangle = 0$, we obtain the surprisingly simple result $\delta h = \sqrt{3x(1-x)}J^{\pm\pm}$ for site dilution [30]. For $\text{Er}_2\text{Ti}_2\text{O}_7$, extensive investigations of the order-by-disorder mechanism estimate $J^{\pm\pm} = 4.2 \times 10^{-2} \text{ meV}$ [12] and $\Delta = 5.3 \times 10^{-2} \text{ meV}$ [35]. To discuss the disappearance of LRO, and given that Eq. (4) is valid at weak disorder only, we instead compare the strength of the fluctuations, δh , to the clean-limit spin gap, Δ , to obtain an upper bound for the critical randomness which reads $\delta h_{\text{cr}} = f\Delta$ where f is a numerical factor of order unity. Experimentally, LRO disappears in $\text{Er}_{2-x}\text{Y}_x\text{Ti}_2\text{O}_7$ around $x_{\text{cr}} \approx 0.15$ [23]; from which we extract $f \approx 1/2$. Evidently, a more quantitative theory is desirable for an accurate determination of x_{cr} – this is left for future work. Our results are applicable to $\text{Er}_2\text{Pt}_2\text{O}_7$ as well, a compound which shows so-called Palmer-Chalker order ($\alpha > 2$) [16], not arising from an order-by-disorder mechanism. Using $f = 1/2$ and experimentally known model parameters, we predict that a small amount of vacancies, $x_{\text{cr}} \approx 4\%$, destabilizes the magnetic order in $\text{Er}_2\text{Pt}_2\text{O}_7$ [30].

Broader aspects of the theory.— Our ideas are of generic relevance to magnets with strong spin-orbit coupling. Key to our scenario is the presence of off-diagonal exchange couplings in the microscopic Hamiltonian. These break spin-rotational invariance, leading to an anisotropy gap in a clean ordered state. In the presence of inhomogeneities, the off-diagonal couplings also produce random fields [32] which compete with the gap (protecting the ordered state) and favor CSG formation instead. The critical level of disorder where LRO disappears is, of course, material-specific.

For the 2D quantum-spin-liquid candidate YbMgGaO_4 [45, 46], it has been argued that quenched disorder in the off-diagonal couplings is responsible for the destruction of LRO [47, 48] due to a “pinning-field” mechanism [48]. According to our scenario, this mechanism is akin to the random-field one which leads to CSG phase. In lower dimensions ($d < 5/2$ [49]), the CSG phase melts into a fluctuating cluster-paramagnet phase, in accordance with the observations in Ref. 48.

Conclusions.— Combining analytical arguments and large-scale MC simulations, we have shown that defects induce fluctuating random fields in XY pyrochlore antiferromagnets. These ultimately destroy magnetic LRO, leading to a CSG phase beyond a critical level of randomness. Our theory resolves the previous discrepancy between theory and experiment, and is in semi-quantitative agreement with experimental data on diluted $\text{Er}_2\text{Ti}_2\text{O}_7$.

We expect our ideas to motivate further studies into the non-trivial role of randomness in magnets with strong spin-orbit coupling, where the presence of off-diagonal ex-

change terms triggers a non-trivial competition between anisotropy gap and random fields [32].

We acknowledge instructive discussions with B. Gaulin, H.-H. Klauss, K. Ross, R. Sarkar, and M. Zhitomirsky. ECA was supported by FAPESP (Brazil) Grant No. 2013/00681-8 and CNPq (Brazil) Grant No. 302065/2016-4. JAH was supported by CNPq Grant No. 307548/2015-5 and FAPESP Grants No. 2015/23849-7 and No. 2016/10826-1. SR and MV were supported by DFG SFB 1143.

-
- [1] J. S. Gardner, M. J. P. Gingras, and J. E. Greedan, “Magnetic pyrochlore oxides,” *Rev. Mod. Phys.* **82**, 53–107 (2010).
- [2] H. Yan, O. Benton, L. Jaubert, and N. Shannon, “Theory of multiple-phase competition in pyrochlore magnets with anisotropic exchange with application to $\text{Yb}_2\text{Ti}_2\text{O}_7$, $\text{Er}_2\text{Ti}_2\text{O}_7$, and $\text{Er}_2\text{Sn}_2\text{O}_7$,” *Phys. Rev. B* **95**, 094422 (2017).
- [3] M. J. Harris, S. T. Bramwell, D. F. McMorrow, T. Zeiske, and K. W. Godfrey, “Geometrical Frustration in the Ferromagnetic Pyrochlore $\text{Ho}_2\text{Ti}_2\text{O}_7$,” *Phys. Rev. Lett.* **79**, 2554–2557 (1997).
- [4] R. Moessner, “Relief and generation of frustration in pyrochlore magnets by single-ion anisotropy,” *Phys. Rev. B* **57**, R5587–R5589 (1998).
- [5] C. L. Henley, “The ‘Coulomb Phase’ in Frustrated Systems,” *Ann. Rev. Cond. Mat. Phys.* **1**, 179–210 (2010).
- [6] C. Castelnovo, R. Moessner, and S.L. Sondhi, “Spin Ice, Fractionalization, and Topological Order,” *Ann. Rev. Cond. Mat. Phys.* **3**, 35–55 (2012).
- [7] M. Hermele, M. P. A. Fisher, and L. Balents, “Pyrochlore photons: The $U(1)$ spin liquid in a $S = \frac{1}{2}$ three-dimensional frustrated magnet,” *Phys. Rev. B* **69**, 064404 (2004).
- [8] K. A. Ross, L. Savary, B. D. Gaulin, and L. Balents, “Quantum Excitations in Quantum Spin Ice,” *Phys. Rev. X* **1**, 021002 (2011).
- [9] M. J. P. Gingras and P. A. McClarty, “Quantum spin ice: a search for gapless quantum spin liquids in pyrochlore magnets,” *Rep. Prog. Phys.* **77**, 056501 (2014).
- [10] J. D. M. Champion, M. J. Harris, P. C. W. Holdsworth, A. S. Wills, G. Balakrishnan, S. T. Bramwell, E. Čížmár, T. Fennell, J. S. Gardner, J. Lago, D. F. McMorrow, M. Orendáč, A. Orendáčová, D. McK. Paul, R. I. Smith, M. T. F. Telling, and A. Wildes, “ $\text{Er}_2\text{Ti}_2\text{O}_7$: Evidence of quantum order by disorder in a frustrated antiferromagnet,” *Phys. Rev. B* **68**, 020401 (2003).
- [11] M. E. Zhitomirsky, M. V. Gvozdikova, P. C. W. Holdsworth, and R. Moessner, “Quantum Order by Disorder and Accidental Soft Mode in $\text{Er}_2\text{Ti}_2\text{O}_7$,” *Phys. Rev. Lett.* **109**, 077204 (2012).
- [12] L. Savary, K. A. Ross, B. D. Gaulin, Jacob P. C. Ruff, and L. Balents, “Order by Quantum Disorder in $\text{Er}_2\text{Ti}_2\text{O}_7$,” *Phys. Rev. Lett.* **109**, 167201 (2012).
- [13] M. E. Zhitomirsky, P. C. W. Holdsworth, and R. Moessner, “Nature of finite-temperature transition in anisotropic pyrochlore $\text{Er}_2\text{Ti}_2\text{O}_7$,” *Phys. Rev. B* **89**, 140403 (2014).
- [14] P. A. McClarty, P. Stasiak, and M. J. P. Gingras, “Order-by-disorder in the XY pyrochlore antiferromagnet,” *Phys. Rev. B* **89**, 024425 (2014).
- [15] B. Javanparast, A. G. R. Day, Z. Hao, and M. J. P. Gingras, “Order-by-disorder near criticality in XY pyrochlore magnets,” *Phys. Rev. B* **91**, 174424 (2015).
- [16] A. M. Hallas, J. Gaudet, N. P. Butch, G. Xu, M. Tachibana, C. R. Wiebe, G. M. Luke, and B. D. Gaulin, “Phase Competition in the Palmer-Chalker XY Pyrochlore $\text{Er}_2\text{Pt}_2\text{O}_7$,” *Phys. Rev. Lett.* **119**, 187201 (2017), 1705.06680.
- [17] J. Villain, R. Bidaux, J.-P. Carton, and R. Conte, “Order as an effect of disorder,” *J. Phys. France* **41**, 1263–1272 (1980).
- [18] E. F. Shender, “Antiferromagnetic garnets with fluctuationally interacting sublattices,” *Sov. Phys. JETP* **56**, 178 (1982).
- [19] C. L. Henley, “Ordering due to disorder in a frustrated vector antiferromagnet,” *Phys. Rev. Lett.* **62**, 2056–2059 (1989).
- [20] J. Villain, “Insulating spin glasses,” *Z. Phys. B* **33**, 31–42 (1979).
- [21] V. S. Maryasin and M. E. Zhitomirsky, “Order from structural disorder in the XY pyrochlore antiferromagnet $\text{Er}_2\text{Ti}_2\text{O}_7$,” *Phys. Rev. B* **90**, 094412 (2014).
- [22] A. Andreanov and P. A. McClarty, “Order induced by dilution in pyrochlore XY antiferromagnets,” *Phys. Rev. B* **91**, 064401 (2015).
- [23] J. Gaudet, A. M. Hallas, D. D. Maharaj, C. R. C. Buhariwalla, E. Kermarrec, N. P. Butch, T. J. S. Munsie, H. A. Dabkowska, G. M. Luke, and B. D. Gaulin, “Magnetic dilution and domain selection in the XY pyrochlore antiferromagnet $\text{Er}_2\text{Ti}_2\text{O}_7$,” *Phys. Rev. B* **94**, 060407 (2016).
- [24] K. A. Ross, J. W. Krizan, J. A. Rodriguez-Rivera, R. J. Cava, and C. L. Broholm, “Static and dynamic XY -like short-range order in a frustrated magnet with exchange disorder,” *Phys. Rev. B* **93**, 014433 (2016).
- [25] R. Sarkar, J. W. Krizan, F. Brückner, E. C. Andrade, S. Rachel, M. Vojta, R. J. Cava, and H.-H. Klauss, “Spin freezing in the disordered pyrochlore magnet $\text{NaCaCo}_2\text{F}_7$: NMR studies and Monte Carlo simulations,” *Phys. Rev. B* **96**, 235117 (2017).
- [26] K. A. Ross, J. M. Brown, R. J. Cava, J. W. Krizan, S. E. Nagler, J. A. Rodriguez-Rivera, and M. B. Stone, “Single-ion properties of the $S_{\text{eff}} = \frac{1}{2}$ XY antiferromagnetic pyrochlores $\text{Na}A'\text{Co}_2\text{F}_7$ ($A' = \text{Ca}^{2+}, \text{Sr}^{2+}$),” *Phys. Rev. B* **95**, 144414 (2017).
- [27] S. H. Curnoe, “Structural distortion and the spin liquid state in $\text{Tb}_2\text{Ti}_2\text{O}_7$,” *Phys. Rev. B* **78**, 094418 (2008).
- [28] J. D. Thompson, P. A. McClarty, H. M. Rønnow, Louis P. Regnault, A. Sorge, and M. J. P. Gingras, “Rods of Neutron Scattering Intensity in $\text{Yb}_2\text{Ti}_2\text{O}_7$: Compelling Evidence for Significant Anisotropic Exchange in a Magnetic Pyrochlore Oxide,” *Phys. Rev. Lett.* **106**, 187202 (2011).
- [29] L. Savary and L. Balents, “Coulombic Quantum Liquids in Spin-1/2 Pyrochlores,” *Phys. Rev. Lett.* **108**, 037202 (2012).
- [30] See Supplemental Material at XXX, which includes Refs. [50–52], for more details on the calculation of the variance of the local exchange field and further classical Monte Carlo results.
- [31] A. Aharony, “Absence of Ferromagnetic Long Range Order in Random Isotropic Dipolar Magnets and in similar

- systems,” *Solid State Commun.* **28**, 667–670 (1978).
- [32] The h_j^\pm take the role of random *fields* in an assumed ordered state, but at the Hamiltonian level disorder results in random *anisotropies*, as time-reversal symmetry is not broken.
- [33] We have assumed uncorrelated disorder which generically applies to the long-wavelength limit.
- [34] Y. Imry and S-k Ma, “Random-Field Instability of the Ordered State of Continuous Symmetry,” *Phys. Rev. Lett.* **35**, 1399–1401 (1975).
- [35] K. A. Ross, Y. Qiu, J. R. D. Copley, H. A. Dabkowska, and B. D. Gaulin, “Order by Disorder Spin Wave Gap in the XY Pyrochlore Magnet $\text{Er}_2\text{Ti}_2\text{O}_7$,” *Phys. Rev. Lett.* **112**, 057201 (2014).
- [36] D. S. Fisher, “Random fields, random anisotropies, nonlinear σ models, and dimensional reduction,” *Phys. Rev. B* **31**, 7233–7251 (1985).
- [37] T. C. Proctor, D. A. Garanin, and E. M. Chudnovsky, “Random Fields, Topology, and the Imry-Ma Argument,” *Phys. Rev. Lett.* **112**, 097201 (2014).
- [38] T. C. Proctor and E. M. Chudnovsky, “Effect of a dilute random field on a continuous-symmetry order parameter,” *Phys. Rev. B* **91**, 140201 (2015).
- [39] The present glass state is fundamentally different from those proposed for the Ising and the isotropic Heisenberg pyrochlores [53, 54]. In those examples, the glassiness is due to effective moments which interact via a spin-liquid background. In contrast, in our case the CSG is due to domain formation.
- [40] J. Lou, A. W. Sandvik, and L. Balents, “Emergence of U(1) Symmetry in the 3D XY Model with Z_q Anisotropy,” *Phys. Rev. Lett.* **99**, 207203 (2007).
- [41] S. Wenzel and A. M. Läuchli, “Unveiling the Nature of Three-Dimensional Orbital Ordering Transitions: The Case of e_g and t_{2g} Models on the Cubic Lattice,” *Phys. Rev. Lett.* **106**, 197201 (2011).
- [42] J. H. Pixley and A. P. Young, “Large-scale Monte Carlo simulations of the three-dimensional XY spin glass,” *Phys. Rev. B* **78**, 014419 (2008).
- [43] N. Todoroki and S. Miyashita, “Ordered Phases and Phase Transitions in The Stacked Triangular Antiferromagnet CsCoCl_3 and CsCoBr_3 ,” *J. Phys. Soc. Jpn.* **73**, 412 (2004).
- [44] K. H. Fischer and J. A. Hertz, *Spin Glasses* (Cambridge University Press, Cambridge, 1991).
- [45] Y. Li, G. Chen, W. Tong, L. Pi, J. Liu, Z. Yang, X. Wang, and Q. Zhang, “Rare-Earth Triangular Lattice Spin Liquid: A Single-Crystal Study of YbMgGaO_4 ,” *Phys. Rev. Lett.* **115**, 167203 (2015).
- [46] J. A. M. Paddison, M. Daum, Z. Dun, G. Ehlers, Y. Liu, M. B. Stone, H. Zhou, and M. Mourigal, “Continuous excitations of the triangular-lattice quantum spin liquid YbMgGaO_4 ,” *Nat. Phys.* **13**, 117–122 (2017).
- [47] Y. Li, D. Adroja, R. I. Bewley, D. Voneshen, A. A. Tsirlin, P. Gegenwart, and Q. Zhang, “Crystalline Electric-Field Randomness in the Triangular Lattice Spin-Liquid YbMgGaO_4 ,” *Phys. Rev. Lett.* **118**, 107202 (2017).
- [48] Z. Zhu, P. A. Maksimov, S. R. White, and A. L. Chernyshev, “Disorder-induced Mimicry of a Spin Liquid in YbMgGaO_4 ,” *Phys. Rev. Lett.* **119**, 157201 (2017).
- [49] A. Maiorano and G. Parisi, “New support for the value 5/2 for the spin glass lower critical dimension at zero magnetic field,” ArXiv e-prints (2017), [arXiv:1711.05590](https://arxiv.org/abs/1711.05590).
- [50] J. L. Alonso, A. Tarancón, H. G. Ballesteros, L. A. Fernández, V. Martín-Mayor, and A. Muñoz Sudupe, “Monte Carlo study of O(3) antiferromagnetic models in three dimensions,” *Phys. Rev. B* **53**, 2537 (1996).
- [51] K. Hukushima and K. Nemoto, “Exchange Monte Carlo Method and Application to Spin Glass Simulations,” *J. Phys. Soc. Jpn.* **65**, 1604 (1996).
- [52] A. K. Hartmann and A. P. Young, “Specific-heat exponent of random-field systems via ground-state calculations,” *Phys. Rev. B* **64**, 214419 (2001).
- [53] T. E. Saunders and J. T. Chalker, “Spin Freezing in Geometrically Frustrated Antiferromagnets with Weak Disorder,” *Phys. Rev. Lett.* **98**, 157201 (2007).
- [54] A. Andreanov, J. T. Chalker, T. E. Saunders, and D. Sherrington, “Spin-glass transition in geometrically frustrated antiferromagnets with weak disorder,” *Phys. Rev. B* **81**, 014406 (2010).

Supplementary information for: Cluster-glass phase in pyrochlore XY antiferromagnets with quenched disorder

Eric C. Andrade,¹ José A. Hoyos,¹ Stephan Rachel,^{2,3} and Matthias Vojta²

¹*Instituto de Física de São Carlos, Universidade de São Paulo, C.P. 369, São Carlos, SP, 13560-970, Brazil*

²*Institut für Theoretische Physik, Technische Universität Dresden, 01062 Dresden, Germany*

³*School of Physics, University of Melbourne, Parkville, Victoria 3010, Australia*

(Dated: April 6, 2024)

I. VARIANCE OF THE LOCAL EXCHANGE FIELD

If we assume long-range order (LRO) which is uniform in the local frames of the Hamiltonian (1) in the main text, with $|\alpha| < 2$, we can write the spin average as $\langle \mathbf{S} \rangle = \langle S^x \rangle \hat{x} + \langle S^y \rangle \hat{y} = m \hat{n}_{\parallel}$. The local exchange field is then given by

$$\mathbf{h}_j = \sum_{k=1}^z (J_{jk}^{xx} \langle S^x \rangle + J_{jk}^{xy} \langle S^y \rangle) \hat{x} + (J_{jk}^{yy} \langle S^y \rangle + J_{jk}^{yx} \langle S^x \rangle) \hat{y}, \quad (\text{S1})$$

with the sum running over all the $z = 6$ nearest-neighbor (NN) sites. In the presence of random off-diagonal exchange couplings the local exchange field $\mathbf{h}_j = h_j^{\parallel} \hat{n}_{\parallel} + h_j^{\perp} \hat{n}_{\perp}$ is not parallel to the mean magnetization, where we defined the transverse direction as $\hat{n}_{\perp} = (-\langle S^y \rangle \hat{x} + \langle S^x \rangle \hat{y})/m$. The general expression for the local transverse component is

$$\begin{aligned} \frac{h_j^{\perp}}{J^{\pm\pm}} &= \frac{2}{m} \sum_{k=1}^z \epsilon_{jk} \sin \theta_{jk} \left(\langle S^x \rangle^2 - \langle S^y \rangle^2 \right) \\ &\quad - \frac{4}{m} \sum_{k=1}^z \epsilon_{jk} \cos \theta_{jk} \langle S^x \rangle \langle S^y \rangle. \end{aligned} \quad (\text{S2})$$

We now make two assumptions: (i) the magnetization m is uniform and (ii) $m = \langle S^x \rangle = \frac{1}{2}$ and thus $\langle S^y \rangle = 0$. Assumption (i) is motivated by the fact that we are interested in the stability of the uniform long-range order, and (ii) is made for simplicity. Equation (S2) then becomes

$$u_j = \frac{h_j^{\perp}}{J^{\pm\pm}} = \sum_{k=1}^6 \epsilon_{jk} \sin \theta_{jk}, \quad (\text{S3})$$

as presented in the main text. Here $\theta_1 = \theta_4 = 0$, $\theta_2 = \theta_5 = \frac{2\pi}{3}$ and $\theta_3 = \theta_6 = -\frac{2\pi}{3}$.

For site dilution we have $\epsilon_{jk} = 0$ if the neighboring site k is occupied, and -1 if vacant. Thus, $\epsilon_{jk} = 0$ with probability $(1-x)$ and -1 with probability x . For bond randomness, on the other hand, $\epsilon_{jk} = +W$ if the coupling with the neighboring site k is the stronger one, and $-W$ (with $0 < W < 1$), for the weaker one. Let x be the concentration of weaker bond, then $\epsilon_{jk} = +W$ with probability $(1-x)$ and $-W$ with probability x . Here, the similarity between bond randomness and site dilution becomes apparent.

We now calculate the possible values of u and their corresponding probabilities considering a fixed number of neighboring impurities (from one to five) uniformly distributed (we drop the site index j in the following discussion). For a single impurity we obtain three values: $u = \pm\omega, 0$, with $\omega = \frac{\sqrt{3}}{2}$ for vacancies and $\omega = \sqrt{3}W$ for bond defects, all of them with equal probability, i.e., $P_1(0) = P_1(\pm\omega) = \frac{1}{3}$. For two impurities we then get $u = \pm 2\omega, \pm\omega, 0$ with probabilities $P_2(\pm 2\omega) = \frac{1}{15}$, $P_2(\pm\omega) = \frac{4}{15}$ and $P_2(0) = \frac{1}{3}$, respectively. Repeating this exercises for three impurities, we find that $P_3(\pm 2\omega) = \frac{1}{10}$, $P_3(\pm\omega) = \frac{1}{5}$, and $P_3(0) = \frac{2}{5}$. For 4 and 5 impurities, we obtain the same results as for 2 and 1 impurities, respectively, i.e., $P_n(u) = P_{6-n}(u)$. Since $P_n(u) = P_n(-u)$, then $\bar{u} = 0$. The variance is

$$\begin{aligned} \overline{u^2} &= \sum_{n=1}^5 \sum_u u^2 P_n(u) \times \binom{6}{n} x^n (1-x)^{6-n} \\ &= 4x(1-x)\omega^2, \end{aligned} \quad (\text{S4})$$

where $\binom{6}{n} x^n (1-x)^{6-n}$ takes into account all possible ways of placing n impurities among the 6 neighboring sites (or sharing bonds). We remark that we are not excluding sites which do not belong to the infinite cluster. This leads to tiny corrections to (S5). Therefore, for site dilution, we get

$$\delta h = \sqrt{u^2} J^{\pm\pm} = \sqrt{3x(1-x)} J^{\pm\pm}, \quad (\text{S5})$$

as stated in the main text, and

$$\delta h = 2\sqrt{3x(1-x)} W J^{\pm\pm} \quad (\text{S6})$$

for bond randomness.

We note that the effective anisotropy energy λ , describing the mean-field selection of ψ_3 , scales with x in the case of dilution and with W^2 in the case of bond disorder [1], such that both cases are expected to display a similar competition between ψ_3 selection and random-field destruction of order, as captured by the stability criterion in Eq. (4) in the main text. However, in our numerical simulations for bond disorder, as described in Sec. III below, we have been unable to find the ψ_3 state for small randomness in the temperature range investigated (in contrast to the case of site dilution). Instead, we observed only the ψ_2 and CSG states even at the classical level.

II. MONTE-CARLO SIMULATION DETAILS

Our Monte-Carlo (MC) simulations are performed on clusters with $N = 4L^3$ spins with periodic boundary conditions and L varying from 6 to 12. We employ three distinct types of MC moves: (a) single-site (restricted) Metropolis updates, (b) microcanonical steps [2] and (c) parallel tempering [3]. Typically, we perform 5×10^5 MC sweeps for thermalization, followed by 5×10^5 sweeps to calculate thermal averages. In our implementation, after 10 microcanonical sweeps we perform a Metropolis sweep followed by a parallel tempering update. For the restricted Metropolis step, we use a temperature-dependent selection window to ensure an average acceptance rate larger than 50% at any given temperature. Moreover, we select our temperature grid such that a parallel tempering move has a success rate larger than 40%. On top of thermal averages, we also perform average typically from over 1 000 defects configurations for $L = 6$ down to 300 configurations for $L = 12$.

In our MC simulations the spins become frozen at low temperature, with non-vanishing expectation values, $\langle \mathbf{S}_i \rangle \neq 0$. If all spins point along the same local direction, we then have $\mathbf{M} = N^{-1} \sum_i \langle \mathbf{S}_i \rangle \neq 0$ which signals LRO. On the other hand, if the spins are frozen in a disordered configuration as in a spin glass we have $\mathbf{M} = 0$. In order to detect spin freezing, independently of LRO, we introduce the Edwards-Anderson order parameter [4, 5]

$$\tilde{q}^{\alpha,\beta} = \overline{N^{-1} \sum_i \langle S_i^\alpha \rangle \langle S_i^\beta \rangle}, \quad (\text{S7})$$

where $\alpha, \beta = x, y, z$ are the spin components and the overline denotes average over disorder. Within the MC simulation, the thermal averages are replaced by averages over MC time, and we get

$$\tilde{q}^{\alpha,\beta} = \overline{N^{-1} \sum_i \mathcal{M}^{-2} \sum_{t_1, t_2} S_i^\alpha(t_1) S_i^\beta(t_2)}, \quad (\text{S8})$$

where \mathcal{M} is the number of Monte Carlo steps. In general, $S_i^\alpha(t_1)$ and $S_i^\beta(t_2)$ have different configurations, and it is then convenient to independently simulate two copies of the system with identical defect configuration (two replicas)

$$\tilde{q}^{\alpha,\beta} = \overline{\mathcal{M}^{-1} \sum_t N^{-1} \sum_i S_i^{\alpha(1)}(t) S_i^{\beta(2)}(t)} \quad (\text{S9})$$

$$= \left\langle \overline{N^{-1} \sum_i S_i^{\alpha(1)} S_i^{\beta(2)}} \right\rangle. \quad (\text{S10})$$

Finally, it is convenient to introduce a \mathbf{q} -dependent Edwards-Anderson order parameter

$$q^{\alpha,\beta}(\mathbf{q}) = \frac{1}{N} \sum_i S_i^{\alpha(1)} S_i^{\beta(2)} e^{i\mathbf{q} \cdot \mathbf{r}_i}, \quad (\text{S11})$$

which is the expression presented in the main text. The spin-glass susceptibility is then given by

$$\chi_{SG}(\mathbf{q}) = N \sum_{\alpha,\beta} \overline{\langle |q^{\alpha,\beta}(\mathbf{q})|^2 \rangle}. \quad (\text{S12})$$

III. ADDITIONAL NUMERICAL RESULTS

A. Bond disorder

In order to simulate bond defects, we consider a binary distribution of bonds strengths described by ϵ_{jk} in Eq. (3) of the main text taking values $+W$ or $-W$ with equal probability. This choice is inspired by the experimental situation in $\text{NaCaCo}_2\text{F}_7$ [6, 7] and $\text{NaSrCo}_2\text{F}_7$ [8].

Sample results are displayed in Figs. S1–S3. The freezing temperature T_f is obtained studying the crossing point of the spin-glass correlation length ξ_{SG} divided by the system size L , as a function of T , as shown in the insets of Figs. S1(a) and S1(b). In Fig. S1 we clearly see that the specific heat becomes more glass-like with increasing W , i.e., the maxima of $C(T)$ become broad and L -independent, characteristic of short-range magnetic correlations building up above T_f [4], as in the case of site dilution. In Fig. S2(a) we present the magnetic correlation length ξ^\perp , divided by the system size L , as a function of T for strong bond disorder $W = 0.9$. The absence of a crossing point indicates the lack of magnetic LRO, which is in accordance with the monotonic suppression of the magnetic order parameter m as L increases [see the inset of Fig. S2(a)]. Moreover, ξ^\perp/L saturates at low temperatures due to the formation of finite-size domains. To further illustrate the glassy behavior, we show in Fig. S2(b) the clock-like order parameter $m_6 = m \cos(6\varphi)$ as a function of T for 80 different bond defect configurations. It is clear that no particular magnetically ordered state is selected since $\overline{\langle m_6 \rangle} \approx 0$ in the temperature window investigated (down to $T \approx T_f/2$). Therefore, similar to the case of site dilution, a CSG phase emerges for large structural defect concentration as the local random-field fluctuations win over the LRO and break the system into domains.

For smaller disorder strength W the situation appears, however, somewhat different compared to the site-diluted case. Here, our Monte-Carlo simulations find no evidence of a ψ_3 phase down to temperatures $T_f/4$, see Fig. S2(c). For $W \leq 0.10$ we always observe $\overline{\langle m_6 \rangle} > 0$, with $\overline{\langle m_6 \rangle}$ monotonically decreasing as we increase W . This implies that the ψ_3 phase in the phase diagram, see Fig. 1(a) of the main text, either exists only at very low temperatures or is absent entirely. In the temperature range probed, we always observe a direct transition from ψ_2 to CSG as W increases. This apparent difference between site dilution and bond disorder may be related to our specific choice of binary bond disorder. Perhaps a different type of dis-

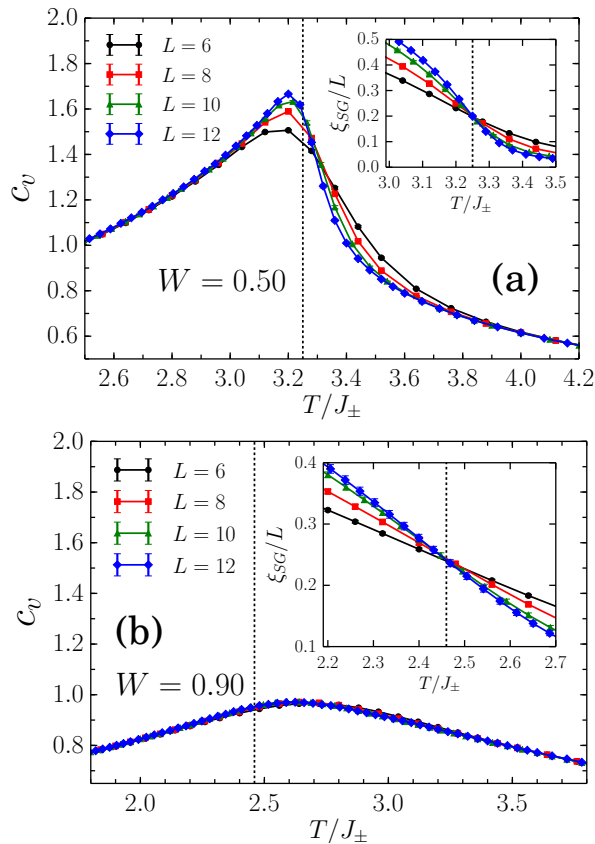


Figure S1. Classical MC results for the Hamiltonian (1) of the main text for off-diagonal exchange ratio $\alpha = 1$ and bond disorder. (a) Specific heat c_v as a function of temperature T for bond disorder $W = 0.5$. (b) Same as (a), but for $W = 0.9$. Inset: spin-glass correlation length divided by the system size ξ_{SG}/L as a function of T showing a crossing point at $T_f/J_{\pm} = 3.25(2)$ and $2.46(2)$ for $W = 0.5$ and 0.9 , respectively.

order distribution, e.g. box disorder [1], would be able to induce a more prominent ψ_3 phase, although earlier MC simulations by some of us also did not find it [7]. At this point we note that, in principle, a different behavior of site and bond dilution close to the homogeneous limit cannot be excluded [9], since a missing site can be seen as $z = 6$ NN weak bonds coupled to a given site, a configuration which occurs with probability $(1/2)^6 = 0.016$ for the current choice of parameters. We postpone a more detailed investigation of the weakly inhomogeneous regime, and the associated peculiar response of a given defect distribution, to a future publication.

The two-dimensional order-parameter distribution $P(m_x, m_y)$ is shown in Fig. S3. In the clean case, $W = 0$, the MC simulations nicely capture the six peaks corresponding to the ψ_2 state. In contrast, for large W we observe the formation of clusters corresponding to several magnetic states, not restricted to ψ_2 and ψ_3 , and no well-separated sharp peaks are formed. These findings are in accordance with our CSG scenario, since the

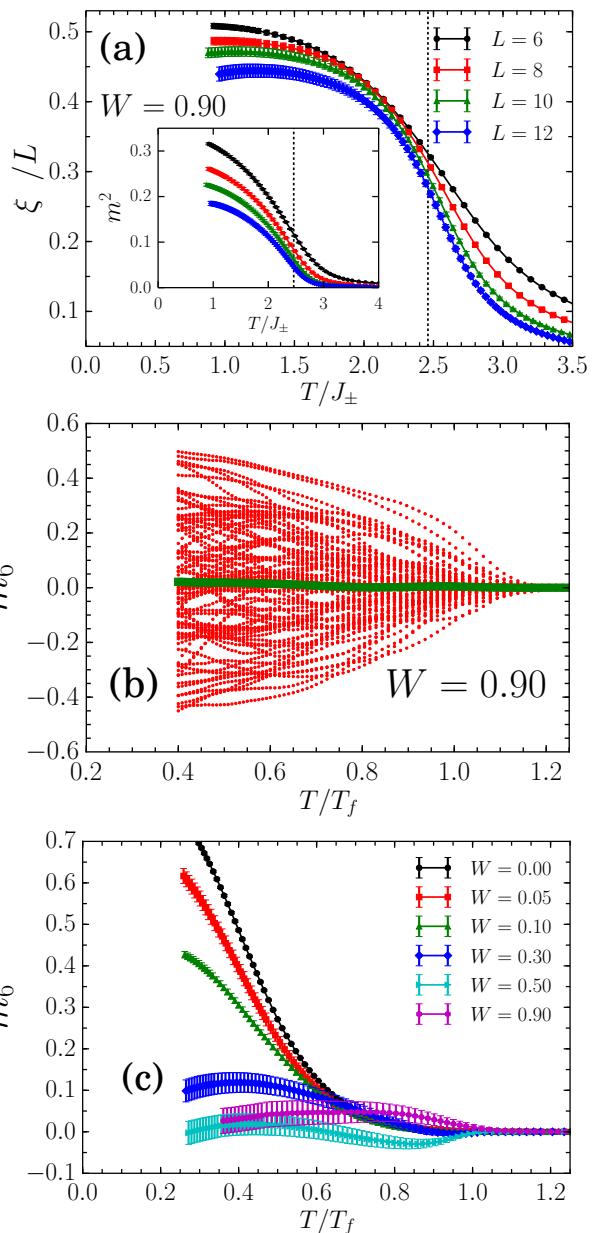


Figure S2. Classical MC results for the Hamiltonian (1) of the main text for off-diagonal exchange ratio $\alpha = 1$ and bond disorder. (a) Magnetic correlation length plotted as $\xi^{-1}(T)/L$ for $W = 0.9$. Inset: square of the magnetic order parameter as a function of T . (b) Clock order parameter m_6 (green squares; error bars are smaller than the symbol size) as a function of T/T_f for $L = 12$ and $W = 0.9$. The result for 80 different defect configurations (red dots) are also shown in order to illustrate the large sample-to-sample fluctuations. (c) Clock order parameter m_6 as a function of T/T_f for five different bond disorder values and $L = 10$.

(local) magnetic order in the clusters is dictated by the local random anisotropies.

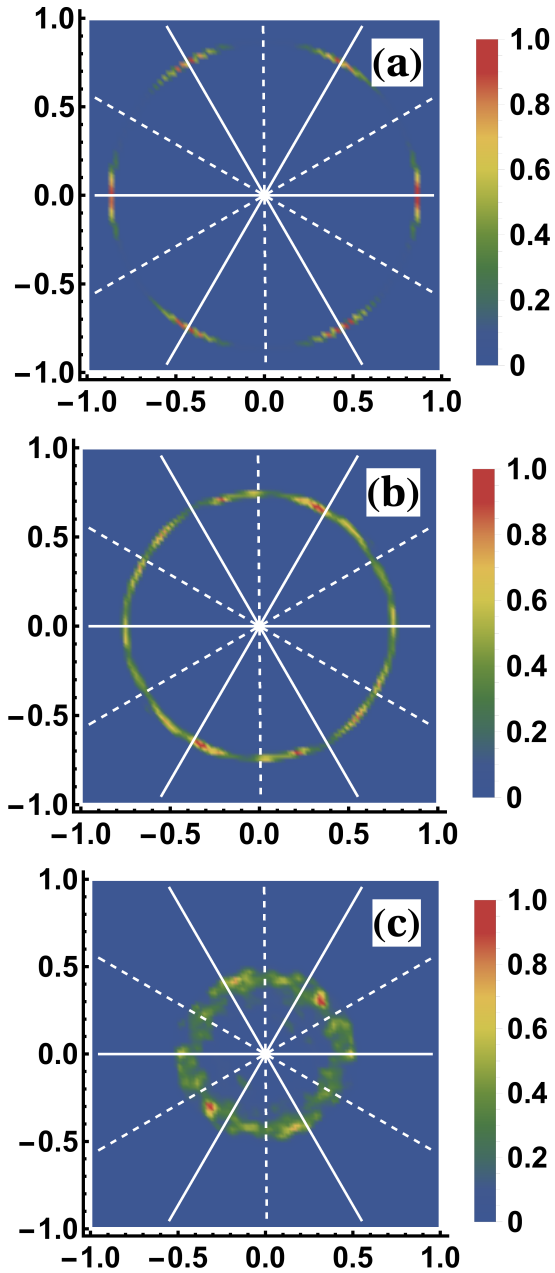


Figure S3. Sample-to-sample distribution function $P(m_x, m_y)$ at $T = T_f/2$ for $L = 12$ obtained via classical Monte Carlo simulation of the Hamiltonian (1) of the main text for off-diagonal exchange parameter $\alpha = 1$ with bond disorder (a) $W = 0$ (the clean system, for comparison), (b) $W = 0.5$, and (c) $W = 0.9$. The full (dashed) radial lines show the expected positions of the peaks associated to the $\psi_{2(3)}$ states.

B. Site dilution

In Fig. S4 we show the specific heat curves as a function of the temperature for the case of site dilution. For $x = 0.3$ the specific heat still displays a weak size depen-

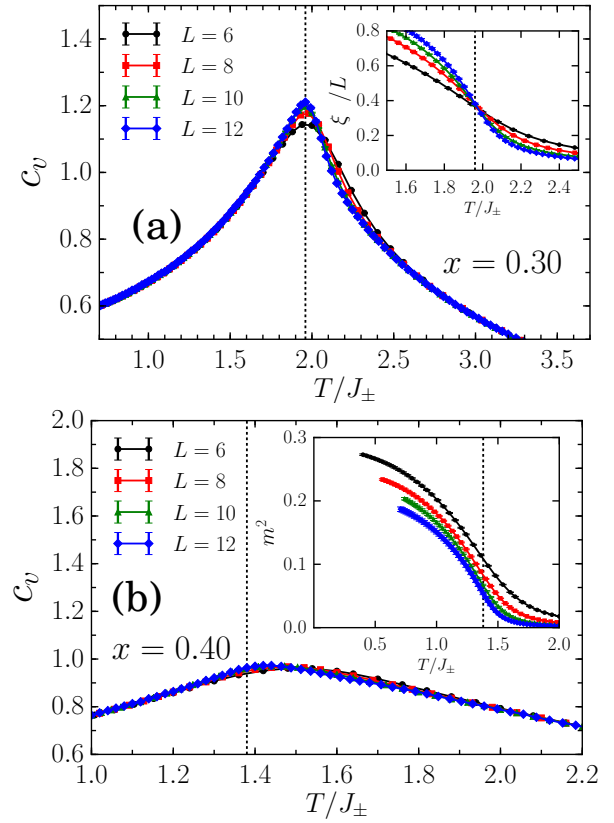


Figure S4. Classical MC results for the Hamiltonian (1) for off-diagonal exchange ratio $\alpha = 1$ and various values of site dilution x . (a,b) Specific heat c_v as a function of temperature T for $x = 0.3$ and $x = 0.4$, respectively. The vertical dashed line marks the position of the freezing temperature T_f . Insets: (a) Magnetic correlation length plotted as $\xi^\perp(T)/L$ for $x = 0.30$, showing a crossing point at $T_f/J_\pm = 1.96(2)$. (b) Square of the magnetic order parameter as a function of T for $x = 0.4$.

dence, and the magnetic correlation length shows a crossing point, indicating that LRO survives, albeit weakly. It eventually disappears around $x_{\text{cr}} \approx 0.35$. As we increase the dilution to $x = 0.4$ both the specific heat and the magnetic order parameter curves exhibit the expected size dependence of a CSG, Fig. S4, which is in accordance with the lack of crossing point in the correlation-length data $\xi^\perp(T)/L$ (Fig. 2(c) of the main text).

In Fig. S5 we present further results for the two-dimensional order parameter distribution $P(m_x, m_y)$, again in the case of site dilution. For the smallest value of dilution studied, $x = 0.1$, our MC results are consistent with the selection of the ψ_3 state, as reported in Refs. 10 and 11 with $P(m_x, m_y)$ displaying well-separated peaks at the positions corresponding to ψ_3 . In contrast, for larger dilution, $x \gtrsim 0.3$, we observe the formation of magnetic clusters containing distinct magnetic states, with the (local) magnetic order in these clusters dictated by the local random anisotropies. This is reflected in

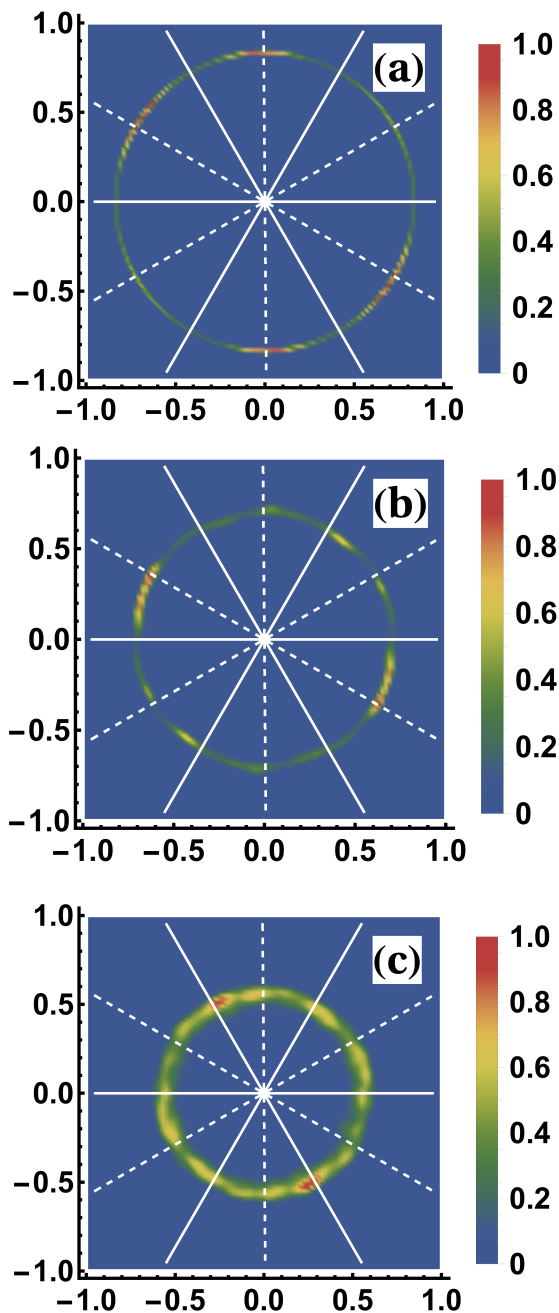


Figure S5. Same as Fig. S3 but for site dilution with concentrations (a) $x = 0.10$, (b) $x = 0.30$, and (c) $x = 0.40$.

$P(m_x, m_y)$ as it both shrinks, signaling a reduction of m , and becomes peaked along a circle.

Summarizing, our classical MC simulations show, for both bond defects and site dilution, the emergence of a CSG phase at large randomness. The glass formation can be attributed to local random exchange fields, which break the system into domains based on energetics.

IV. STABILITY CRITERION AND COMPARISON TO EXPERIMENTS

Here we give some details concerning the analytical calculations and the stability estimates based upon them. We start with the effective field theory employed by Savary *et al.* [12] to describe fluctuations within the classically degenerate manifold of states. This theory is formulated in terms of an angle ϕ where $\phi = \pi n/3$ ($\phi = \pi n/3 + \pi/6$) corresponds to ψ_2 (ψ_3) ordering, respectively. The action reads

$$\mathcal{S} = \int \frac{d^3r}{v_{u.c.}} d\tau \left[\sum_{\mu} \frac{\kappa_{\mu}}{2} (\partial_{\mu}\phi)^2 + \frac{\eta}{2} (\partial_{\tau}\phi)^2 - \frac{\tilde{\lambda}}{2} \cos 6\phi \right]. \quad (\text{S13})$$

Here, κ_{μ} and η are energies characterizing the underlying gradient expansion, and $\tilde{\lambda}$ is an anisotropy energy, for details see the supplement of Ref. 12. Assuming $\tilde{\lambda} > 0$ and expanding in fluctuations around the minimum of the cosine, we find

$$\chi^{\perp}(\mathbf{q}, \omega) = \frac{1}{-\eta\omega^2 + \kappa_{\mu}q_{\mu}^2 + 18\tilde{\lambda}} \quad (\text{S14})$$

as the transverse susceptibility of the ordered ψ_2 state. This matches the expression given in the main text, provided we take the static limit and assign $\lambda = 18\tilde{\lambda}$.

We now calculate the local transverse response due to fluctuating transverse field. As outlined in the main text, we have

$$\overline{\langle S_i^{\perp 2} \rangle} = (\delta h)^2 \int \frac{d^3q}{(2\pi)^3} \chi^{\perp}(\mathbf{q})^2. \quad (\text{S15})$$

Power counting shows that the r.h.s. of this equation scales as $(\delta h)^2 \kappa^{-3/2} \lambda^{-1/2}$ where $\kappa^2 = \sum_{\mu} \kappa_{\mu}^2 / 3$ is the averaged gradient energy. This eventually yields the stability criterion for weak disorder advertised in the main text, Eq. (5), here for $d = 3$.

Since the LRO phase is stable for small disorder, any transition from LRO to CSG has to appear at a finite level of disorder and is hence beyond the linear-response theory used to derive (S15). To estimate the critical level of disorder, we instead revert to a qualitative criterion: Stability of LRO requires that the fluctuating transverse field gap is smaller than the gap protecting the ordered state. By using the gap of the homogeneous reference system, $\Delta = \sqrt{18\tilde{\lambda}/\eta}$, we then obtain an *upper bound* for the stability of LRO

$$\delta h_{\text{cr}} = f\Delta. \quad (\text{S16})$$

Here, δh_{cr} is the critical level of randomness, and simply f is a numerical factor of order unity which we fix by comparing to experimental results and/or numerical calculations.

We may benchmark the idea (S16) using the 3d Ising model in a random longitudinal field. Even though in this

case there are no transverse fluctuations, it is instructive to see if our arguments hold here. The Imry-Ma criterion says that LRO is stable and therefore $\delta h_{\text{cr}} > 0$. For a random field following a Gaussian distribution, careful numerical calculations provide $\delta h_{\text{cr}} = 2.28(1)J$ at $T = 0$ [13]. If we use $\Delta = 12J$ we obtain $f \approx 1/5$ from Eq. (S16), suggesting that the criterion (S16) is reasonable.

We now apply this criterion to available experimental data; the results of this comparison are given in the main text. For $\text{Er}_2\text{Ti}_2\text{O}_7$, an extensive analysis of the order-by-disorder physics in the clean limit has appeared in Ref. 12, yielding the estimate $J^{\pm\pm} = 4.2 \times 10^{-2}$ meV. Inserted into Eq. (S4) we obtain δh as function of dilution level. This needs to be compared to the clean-limit spin gap whose measured value is $\Delta = 5.3 \times 10^{-2}$ meV [14]. Experimentally, LRO disappears in $\text{Er}_{2-x}\text{Y}_x\text{Ti}_2\text{O}_7$ around $x_{\text{cr}} \approx 0.15$ [15]. Inserting this into the criterion (S16) and solving for f we obtain $f \approx 1/2$, again suggesting that the criterion is reasonable. With f fixed for a class of systems, we can now use (S16) for other materials.

In particular, our results should also be applicable to $\text{Er}_2\text{Pt}_2\text{O}_7$, a compound which shows so-called Palmer-Chalker order as $\alpha > 2$ [16], not arising from an order-by-disorder mechanism. It is easy to see that our simple expression for δh also holds in this case. From the phase diagram summarized in Ref. 17 and the transition temperatures for $\text{Er}_2\text{Ti}_2\text{O}_7$ and $\text{Er}_2\text{Pt}_2\text{O}_7$ (1.2 K and 0.38 K, respectively), we extract $\alpha \approx 2.5$ and $J^{\pm\pm} \approx 2.1 \times 10^{-1}$ meV for $\text{Er}_2\text{Pt}_2\text{O}_7$. Using this estimative together with the experimentally reported value of the spin gap, $\Delta = 1.4 \times 10^{-1}$ meV [16], and again $f = 1/2$, we predict that a small amount of vacancies, $x_{\text{cr}} \approx 4\%$, destabilizes the magnetic order in diluted $\text{Er}_2\text{Pt}_2\text{O}_7$. We note that, compared to $\text{Er}_2\text{Ti}_2\text{O}_7$, the larger value of the anisotropic exchange ratio $\alpha = J^{\pm\pm}/J^{\pm}$ enhances the effects of randomness.

[1] V. S. Maryasin and M. E. Zhitomirsky, “Order from structural disorder in the XY pyrochlore antiferromagnet $\text{Er}_2\text{Ti}_2\text{O}_7$,” *Phys. Rev. B* **90**, 094412 (2014).
 [2] J. L. Alonso, A. Taranc3n, H. G. Ballesteros, L. A. Fern3ndez, V. Mart3n-Mayor, and A. Mu3oz Sudupe, “Monte Carlo study of O(3) antiferromagnetic models in three dimensions,” *Phys. Rev. B* **53**, 2537 (1996).
 [3] K. Hukushima and K. Nemoto, “Exchange Monte Carlo

Method and Application to Spin Glass Simulations,” *J. Phys. Soc. Jpn.* **65**, 1604 (1996).
 [4] K. H. Fischer and J. A. Hertz, *Spin Glasses* (Cambridge University Press, Cambridge, 1991).
 [5] J. H. Pixley and A. P. Young, “Large-scale Monte Carlo simulations of the three-dimensional XY spin glass,” *Phys. Rev. B* **78**, 014419 (2008).
 [6] K. A. Ross, J. W. Krizan, J. A. Rodriguez-Rivera, R. J. Cava, and C. L. Broholm, “Static and dynamic XY-like short-range order in a frustrated magnet with exchange disorder,” *Phys. Rev. B* **93**, 014433 (2016).
 [7] R. Sarkar, J. W. Krizan, F. Br3uckner, E. C. Andrade, S. Rachel, M. Vojta, R. J. Cava, and H.-H. Klauss, “Spin freezing in the disordered pyrochlore magnet $\text{NaCaCo}_2\text{F}_7$: NMR studies and Monte Carlo simulations,” *Phys. Rev. B* **96**, 235117 (2017).
 [8] K. A. Ross, J. M. Brown, R. J. Cava, J. W. Krizan, S. E. Nagler, J. A. Rodriguez-Rivera, and M. B. Stone, “Single-ion properties of the $S_{\text{eff}} = \frac{1}{2}$ XY antiferromagnetic pyrochlores $\text{NaA}'\text{Co}_2\text{F}_7$ ($A' = \text{Ca}^{2+}, \text{Sr}^{2+}$),” *Phys. Rev. B* **95**, 144414 (2017).
 [9] C. L. Henley, “Ordering due to disorder in a frustrated vector antiferromagnet,” *Phys. Rev. Lett.* **62**, 2056 (1989).
 [10] M. E. Zhitomirsky, P. C. W. Holdsworth, and R. Moessner, “Nature of finite-temperature transition in anisotropic pyrochlore $\text{Er}_2\text{Ti}_2\text{O}_7$,” *Phys. Rev. B* **89**, 140403 (2014).
 [11] A. Andreanov and P. A. McClarty, “Order induced by dilution in pyrochlore XY antiferromagnets,” *Phys. Rev. B* **91**, 064401 (2015).
 [12] L. Savary, K. A. Ross, B. D. Gaulin, J. P. C. Ruff, and L. Balents, “Order by Quantum Disorder in $\text{Er}_2\text{Ti}_2\text{O}_7$,” *Phys. Rev. Lett.* **109**, 167201 (2012).
 [13] A. K. Hartmann and A. P. Young, “Specific-heat exponent of random-field systems via ground-state calculations,” *Phys. Rev. B* **64**, 214419 (2001).
 [14] K. A. Ross, Y. Qiu, J. R. D. Copley, H. A. Dabkowska, and B. D. Gaulin, “Order by Disorder Spin Wave Gap in the XY Pyrochlore Magnet $\text{Er}_2\text{Ti}_2\text{O}_7$,” *Phys. Rev. Lett.* **112**, 057201 (2014).
 [15] J. Gaudet, A. M. Hallas, D. D. Maharaj, C. R. C. Buhariwalla, E. Kermarrec, N. P. Butch, T. J. S. Munsie, H. A. Dabkowska, G. M. Luke, and B. D. Gaulin, “Magnetic dilution and domain selection in the XY pyrochlore antiferromagnet $\text{Er}_2\text{Ti}_2\text{O}_7$,” *Phys. Rev. B* **94**, 060407 (2016).
 [16] A. M. Hallas, J. Gaudet, N. P. Butch, G. Xu, M. Tachibana, C. R. Wiebe, G. M. Luke, and B. D. Gaulin, “Phase Competition in the Palmer-Chalker XY Pyrochlore $\text{Er}_2\text{Pt}_2\text{O}_7$,” *Phys. Rev. Lett.* **119**, 187201 (2017).
 [17] H. Yan, O. Benton, L. Jaubert, and N. Shannon, “Theory of multiple-phase competition in pyrochlore magnets with anisotropic exchange with application to $\text{Yb}_2\text{Ti}_2\text{O}_7$, $\text{Er}_2\text{Ti}_2\text{O}_7$, and $\text{Er}_2\text{Sn}_2\text{O}_7$,” *Phys. Rev. B* **95**, 094422 (2017).